Telomere anchoring at the nuclear periphery requires the budding yeast Sad1-UNC-84 domain protein Mps3

Jennifer M. Bupp,[1] Adriana E. Martin,[1] Elizabeth S. Stensrud,[1] and Sue L. Jaspersen[1,2]

[1]Stowers Institute for Medical Research, Kansas City, MO 64110
[2]Department of Biochemistry and Molecular Biology, University of Kansas Medical Center, Kansas City, KS 66160

Positioning of telomeres at the nuclear periphery can have dramatic effects on gene expression by establishment of heritable, transcriptionally repressive subdomains. However, little is known about the integral membrane proteins that mediate telomere tethering at the nuclear envelope. Here, we find a previously unrecognized function for the *Saccharomyces cerevisiae* Sad1-UNC-84 domain protein Mps3 in regulating telomere positioning in mitotic cells. Our data demonstrate that the nucleoplasmic N-terminal acidic domain of Mps3 is not essential for viability. However, this acidic domain is necessary and sufficient for telomere tethering during S phase and the silencing of reporter constructs integrated at telomeres. We show that this is caused by the role of the Mps3 acidic domain in binding and localization of the silent information regulator protein Sir4 to the nuclear periphery. Thus, Mps3 functions as an integral membrane anchor for telomeres and is a novel nuclear receptor for the Sir4 pathway of telomere tethering and gene inactivation.

Introduction

The three-dimensional organization of chromosomes within the nucleus of many organisms is nonrandom. Changes in chromosome position can have dramatic effects on gene expression by the establishment and maintenance of heritable transcriptionally repressive or active subdomains (Taddei et al., 2004b; Akhtar and Gasser, 2007; Fraser and Bickmore, 2007). The relationship between nuclear positioning and the epigenetic control of gene expression has perhaps been best characterized in *Saccharomyces cerevisiae* at the telomeres, where their localization at the nuclear periphery has been associated with transcriptional repression (for reviews see Rusche et al., 2003; Moazed et al., 2004; Akhtar and Gasser, 2007).

Yeast telomeres form a compact chromatin structure that not only protects the chromosome ends but also represses the transcription of adjacent genes by RNA polymerase II in a stable, heritable manner termed the telomere position effect (Gottschling et al., 1990). Telomeric silencing requires the silent information regulator (SIR) proteins Sir3 and 4, the NAD$^+$-dependent histone deacetylase Sir2, and the heterodimeric proteins yKu70 and yKu80

in addition to several telomere-binding proteins (Rusche et al., 2003; Moazed et al., 2004). During S phase, both Sir4 and yKu70–yKu80 link telomeric heterochromatin to the nuclear envelope via interactions with Esc1, a large acidic protein located on the nucleoplasmic face of the inner nuclear membrane (Andrulis et al., 1998; Hediger et al., 2002; Gartenberg et al., 2004; Taddei et al., 2004a). However, the yKu70–yKu80 complex also interacts with another, unknown perinuclear factor during G1 (Hediger et al., 2002; Taddei et al., 2004a). Although telomeres frequently cluster near the nuclear periphery, it is not absolutely required for transcriptional inactivation of telomeric or subtelomeric genes (Gotta et al., 1996; Maillet et al., 1996, 2001; Taddei et al., 2004a). Instead, nuclear anchoring might promote gene repression by creating zones with high local concentrations of silencing factors.

Despite our considerable knowledge of proteins involved in the telomere position effect, integral membrane anchors for either the yKu70–yKu80 or Sir4–Esc1 pathways are unknown. Sad1-UNC-84 (SUN) domain proteins are excellent candidates to play a role in connecting telomeres with the nuclear envelope. These integral membrane proteins are present in the inner nuclear envelope of virtually all eukaryotes, with the conserved C-terminal SUN domain located in the space between the inner and outer nuclear membranes and the divergent N termini located in the nucleoplasm (for review see Starr and Fischer, 2005; Tzur et al., 2006; Worman and Gundersen, 2006). Recently, SUN proteins
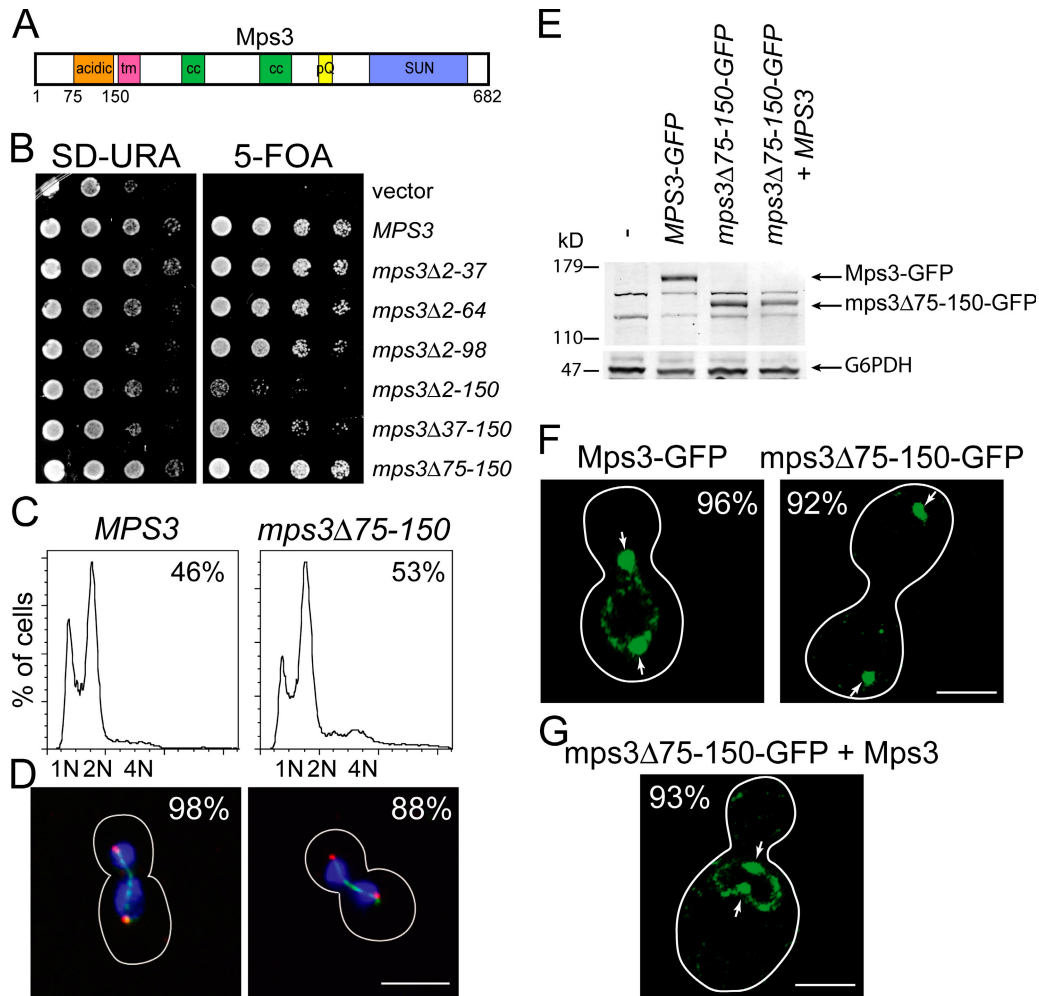
Figure 1. **The Mps3 acidic domain is required for peripheral nuclear envelope localization.** (A) Schematic of Mps3 showing the acidic domain from amino acids 75–150 as well as the transmembrane domain (tm), regions of coiled-coil (cc), the polyglutamine repeat (pQ), and the SUN domain. (B) Versions of *MPS3* in which the indicated N-terminal amino acids were deleted were constructed and transformed into SLJ2039 along with an empty vector and wild-type *MPS3*. The ability of each to rescue *mps3Δ* was tested by plating fivefold serial dilutions to 5-FOA. Cells were also stamped to SD-URA. Plates were incubated for 2 d at 30°C. (C) *MPS3* (SLJ2059) and *mps3Δ75–150* (SLJ2064) cells were grown to mid-log phase at 30°C. Flow cytometric analysis of DNA content and quantitation of budding index indicated that *mps3Δ75–150* mutants do not arrest in mitosis. The biphasic peaks represent cells with G1 (1 N) and G2/M (2 N) DNA content. The percentage of large-budded cells in each sample is indicated. (D) Indirect immunofluoroescence was performed to visualize microtubules (green), SPBs (anti-Tub4; red), and DNA (DAPI; blue). The percentage of large-budded cells with bipolar mitotic spindles was determined by counting the number of Tub4 signals per cell (*n* = 200). (E) Protein levels in extracts of wild-type (SLJ001), *MPS3-GFP* (SLJ2551), *mps3Δ75–150–GFP* (SLJ2552), and *mps3Δ75–150–GFP MPS3* (SLJ2659) cells were determined by Western blotting with anti-GFP antibodies. Glucose–6-phosphate dehydrogenase served as a loading control. (F) Localization of Mps3-GFP and *mps3Δ75–150–GFP* (green) was determined by confocal imaging of yeast nuclei using avalanche photodiode detectors. Projection images were generated as described in Materials and methods. Arrows indicate the position of SPBs and the percentages indicate the proportion of cells observed with the localization pattern presented. (G) We also examined *mps3Δ75–150–GFP* localization in cells containing a wild-type copy of *mps3* (SLJ2659). Bars, 5 μm.

have been shown to bind to meiosis-specific telomere-binding proteins and play a role in the formation of the meiotic bouquet, a specialized clustering of telomeres at the nuclear envelope that occurs before meiosis I (Chikashige et al., 2006; Tang et al., 2006; Conrad et al., 2007; Ding et al., 2007; Penkner et al., 2007; Schmitt et al., 2007). The yeast SUN protein Mps3 has been shown to play a role in telomere clustering in mitotic cells (Antoniacci et al., 2007), suggesting that SUN proteins may also play a role in telomere tethering at the nuclear membrane during mitotic growth.

We generated mutants in the N-terminal acidic domain of Mps3 and found that this domain is not essential for viability or Mps3's known function in spindle pole body (SPB) duplication (Jaspersen et al., 2002; Nishikawa et al., 2003). Instead, we found that the Mps3 N-terminal acidic domain functions to

anchor chromosome arms at the nuclear envelope through the Sir4 pathway of telomere tethering. Thus, telomere positioning at the nuclear membrane is a conserved function that Mps3 plays in both mitotic and meiotic cells. The fact that mutants in the Mps3 N terminus also display defects in proper localization of Sir4 to the nuclear periphery and in telomeric silencing indicates that Mps3 likely functions as a nuclear membrane receptor for the SIR complex, which includes Sir4.

Results

Mps3 N-terminal mutants

To examine the role of Mps3 in telomere tethering during mitotic growth, we constructed a series of deletion mutants in the
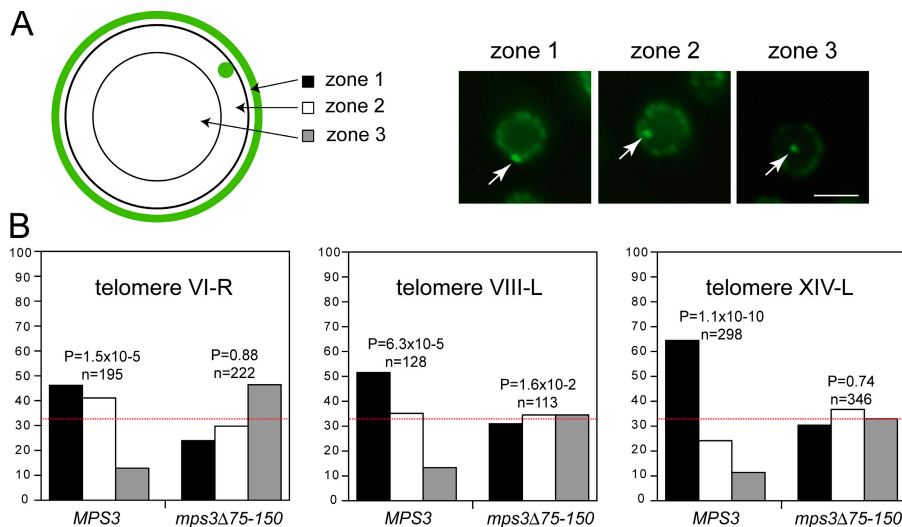
Figure 2. **mps3Δ75–150 mutants have defects in telomere tethering.** (A) Yeast cells expressing GFP-LacI and Nup49-GFP fusions were tagged with ∼256 copies of the LacO$_R$ at telomere VI-R, VIII-L, or XIV-L. The subnuclear position of the telomere was scored with respect to the distance from the nuclear envelope in a single plane image and assigned a position into one of three zones of equal volume (see text for details). Bar, 5 μm. (B) The distribution of telomere ends in zone 1 (black), 2 (white), and 3 (gray) was determined in asynchronously growing wild-type and mps3Δ75–150 cells at 30°C for each telomere. The dotted line at 33% corresponds to a random distribution. Confidence values (P) for the χ^2 test were calculated for each dataset between random and test distributions. The number of cells examined in each dataset is indicated (n).

nucleoplasmic Mps3 N terminus (Fig. 1 A) and transformed them into the *LEU2* locus of a strain containing a complete deletion of the chromosomal copy of *MPS3*. These cells were kept alive by *MPS3* on a centromeric *URA3*-marked plasmid. By plating cells to 5-fluoroorotic acid (5-FOA), we could select for loss of the *URA3* plasmid containing *MPS3* and analyze the growth phenotype of the N-terminal deletion mutants. We found that the Mps3 N terminus is not required for viability (Fig. 1 B), although its complete elimination (amino acids 2–150) did result in reduced fitness, SPB duplication defects, and a temperature-sensitive growth phenotype (not depicted).

Deletion of the acidic region in the Mps3 N terminus (amino acids 75–150) did not result in any apparent growth abnormalities nor did cells display defects in SPB duplication (Fig. 1, B–D). It also did not affect localization to the SPB, although levels of *mps3Δ75–150* fused to GFP (*mps3Δ75–150–GFP*) were reduced compared with Mps3-GFP (Fig. 1, E and F). Analysis of the nuclear envelope staining pattern of Mps3-GFP by single photon imaging methods revealed that Mps3-GFP was present in multiple punctuate foci on the nuclear envelope in 96% of cells imaged (n = 93; Fig. 1 F). *mps3Δ75–150–GFP*, however, showed significantly reduced nuclear envelope staining and a decrease in foci formation; only 8% of cells showed any signal in the peripheral nuclear membrane besides the SPB signal (n = 71; Fig. 1 F). Loss of *mps3Δ75–150–GFP* localization to the nuclear envelope was rescued by coexpression of a wild-type, untagged copy of *MPS3* (n = 68; Fig. 1 G), indicating that our inability to detect *mps3Δ75–150–GFP* at the nuclear membrane is not the result of detection methods but rather reflects a requirement for the N-terminal acidic domain in localization of Mps3 to the nuclear periphery.

The Mps3 acidic domain is required for telomere tethering

Using the new *mps3Δ75–150* allele, we could test the requirement of the Mps3 N terminus in telomere tethering at the nuclear periphery. Tandem repeats of the lactose operator (LacO$_R$) were integrated into individual telomeres, and expression of a GFP fusion to the DNA-binding region of the lactose repressor

(GFP-LacI) allowed visualization of the telomeric locus in living cells. The position of each spot relative to the nuclear periphery, as well as nuclear diameter, was monitored by coexpression of the nucleoporin Nup49 fused to GFP (*NUP49-GFP*; Fig. 2 A). By dividing the locus-to-periphery distance by the nuclear diameter, we assigned each spot a position into one of three concentric zones of equal volume that approximates its position within the nucleus (Hediger et al., 2002). Loci in the most peripheral zone (zone 1) are anchored to the nuclear envelope, whereas loci in the intermediate zone (zone 2) region may have partial contacts with the nuclear envelope. The innermost zone (zone 3) contains loci that are not associated with the nuclear periphery.

Examination of LacO$_R$ integrated at telomere VI-R, VIII-L, or XIV-L in wild-type cells revealed the preferential association of telomeres with the nuclear periphery that others have previously observed (Fig. 2 B; Hediger et al., 2002). In *mps3Δ75–150* mutants, the nuclear envelope appeared intact and was similar to wild-type cells based on Nup49-GFP epifluorescence as well as immunofluorescence analysis with other nucleoporin antibodies (unpublished data). However, association of telomeres with the nuclear envelope was lost and chromosome ends assumed a random distribution within the nucleus (Fig. 2 B). The fact that we observed loss of anchoring of all three telomeres, which are known to have different molecular requirements for nuclear envelope association (Hediger et al., 2002), suggests that the Mps3 N terminus plays a fundamental role in telomere tethering at the nuclear periphery.

The Mps3 N terminus is sufficient to restore telomere tethering to mps3Δ75–150 mutants

We expressed Mps3 N-terminal fragments from the *MPS3* promoter in *mps3Δ75–150* mutants to determine the minimal region of Mps3 necessary for recruitment of telomeres to the nuclear periphery (Fig. 3 A). Although none of these N-terminal constructs was able to complement growth of *mps3Δ* cells (not depicted), the soluble Mps3 N-terminal domain consisting of amino acids 1–150, as well as a version of Mps3 containing the entire N terminus
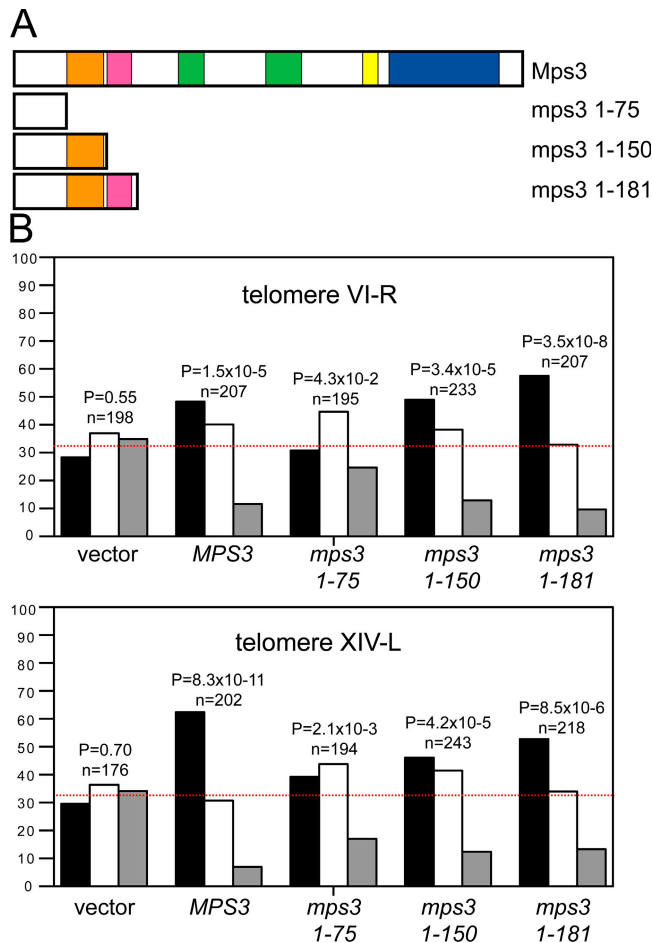
Figure 3. **The Mps3 N terminus is sufficient to restore telomere tethering to *mps3Δ75–150* mutants.** (A) Schematic of Mps3 containing the domains described in Fig. 1 A and constructs containing the indicated regions of the Mps3 N terminus. These were introduced into *mps3Δ75–150* mutants expressing GFP-LacI and Nup49-GFP fusions along with copies of the LacO$_R$ at telomere VI-R or XIV-L. (B) The distribution of telomere ends in zone 1 (black), 2 (white), and 3 (gray) was determined in asynchronously growing cells at 30°C for each telomere. The dotted line at 33% corresponds to a random distribution. Confidence values (P) for the χ^2 test were calculated for each dataset between random and test distributions. The number of cells examined in each dataset is indicated (n).

and the transmembrane domain (*mps3 1–181*), was able to restore tethering of both telomeres VI-R and XIV-L to the nuclear membrane in *mps3Δ75–150* mutants (Fig. 3 B). A version of the Mps3 N terminus lacking the acidic domain (*mps3 1–75*) failed to efficiently anchor telomeres (Fig. 3 B), suggesting that the acidic domain may be involved in an important binding interaction that tethers the chromosome ends at the nuclear periphery. Alternatively, *mps3 1–75* may simply not be targeted correctly to the nucleus, although it is small enough to freely diffuse through nuclear pore complexes.

mps3Δ75–150 mutants are defective in S phase telomere tethering

In G1 phase of the cell cycle, yKu70–yKu80–dependent tethering is the dominant mechanism of nuclear envelope localization of telomeres, whereas binding to the Sir4–Esc1 complex is thought to keep telomeres at the nuclear periphery during S phase
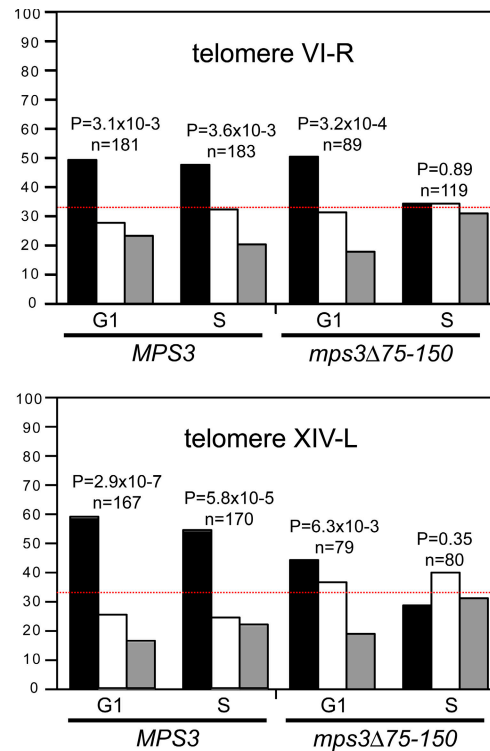

Figure 4. ***mps3Δ75–150* mutants are defective in S phase telomere tethering.** The number of telomere ends in each zone of the nucleus was specifically examined in unbudded G1 cells and small- to medium-budded S-phase cells in an asynchronously growing culture of wild-type and *mps3Δ75–150* mutant cells expressing GFP-LacI and Nup49-GFP fusions along with copies of the LacO$_R$ at telomere VI-R or XIV-L. The dotted line at 33% corresponds to a random distribution. Confidence values (P) for the χ^2 test were calculated for each dataset between random and test distributions. The number of cells examined in each dataset is indicated (n).

(Hediger et al., 2002; Taddei et al., 2004a). We examined recruitment of telomeres VI-R and XIV-L to the nuclear envelope in G1 and S phase cells, which were scored in an asynchronous population of cells based on bud morphology, to determine if the yKu70–yKu80 or Sir4–Esc1 pathway is predominately affected in *mps3Δ75–150* mutants. Over 50 and 44% of G1 *mps3Δ75–150* cells contained telomeres VI-R and XIV-L, respectively, in the outermost zone of the nucleus compared with 34 and 29% of S phase cells (Fig. 4). This suggests that telomere tethering is most affected in S phase cells in *mps3Δ75–150* mutants and that Mps3 is likely involved in the Sir4–Esc1 pathway of telomere recruitment to the nuclear membrane.

The Mps3 acidic domain interacts with Sir4

To test if Mps3 physically interacts with Sir4, Esc1, or yKu70, we immunoprecipitated Mps3 fused at its C terminus to three copies of the HA epitope (Mps3-HA3) from yeast cells that had been lysed after liquid nitrogen grinding and Western blotted with anti-FLAG (to detect yKu70-FLAG3), anti-MYC (to detect Esc1-MYC13), or Sir4 antibodies. Mps3-HA3 bound to Sir4 (Fig. 5 A), but it did not reproducibly bind to Esc1 or yKu70 (not depicted). Binding was dependent on the Mps3 acidic domain, as *mps3Δ75–150–HA3* showed significantly reduced interaction with Sir4 (Fig. 5 A). We were unable to coimmunoprecipitate
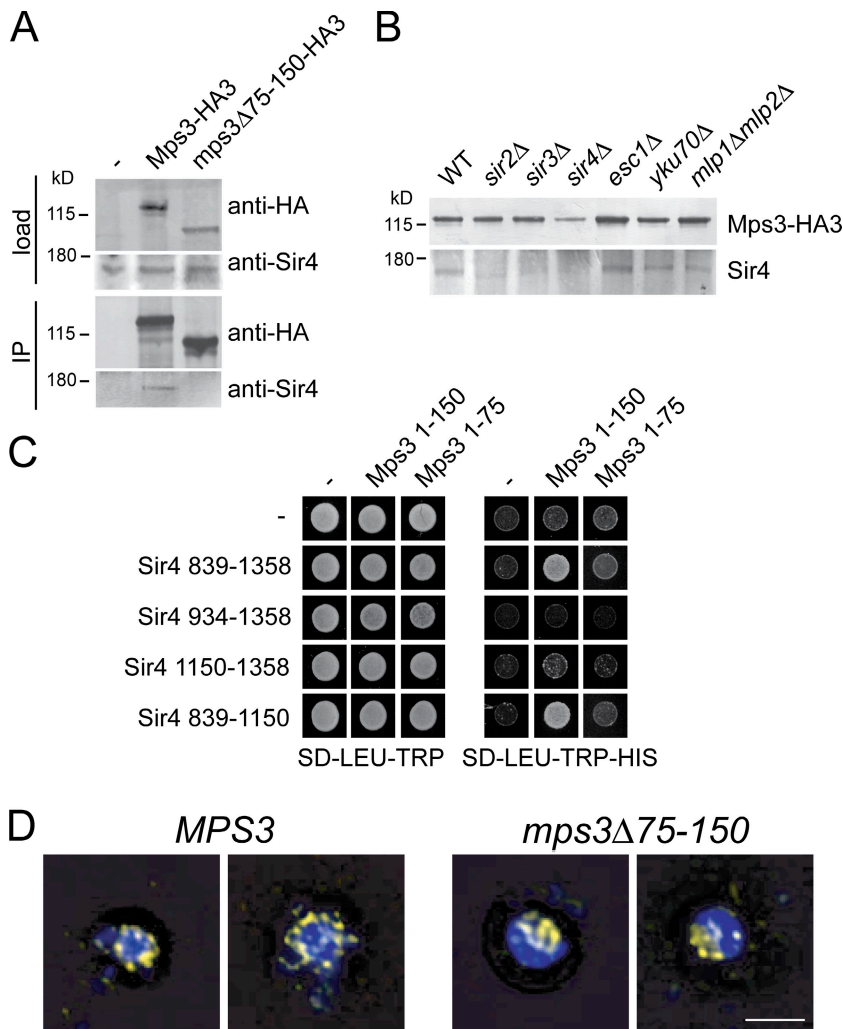
Figure 5. Mps3 interacts with Sir4 through its acidic domain. (A) The protein composition of anti-HA immunoprecipitates from wild-type (SLJ001), *MPS3-HA3* (SLJ922), and *mps3Δ75–150–HA3* (SLJ2529) cells was analyzed by Western blotting with anti-HA and anti-Sir4 antibodies. Lysates were also analyzed directly by Western blotting. (B) Similarly, the protein composition of the anti-HA immunoprecipitates from the indicated deletion strains was analyzed by Western blotting with anti-HA and anti-Sir4 antibodies. (C) Two-hybrid analysis was done with SLJ1644 cells containing the indicated *GAL4*-activation domain fusions (columns) and SLJ1645 cells containing the indicated *GAL4*-DNA binding domain fusions (rows). Diploids were selected on SD-LEU-TRP plates at 30°C, and the ability of fusion proteins to interact was assayed by plating cells, which contain a version of *HIS3* driven by the *GAL1* promoter, on SD-LEU-TRP-HIS plates at 30°C. (D) Localization of Sir4 (anti-Sir4; yellow) and DNA (DAPI; blue) was determined in wild-type (SLJ2059) and *mps3Δ75–150* mutants (SLJ2064) enriched in S phase with hydroxyurea. Bar, *5* μm.

Mps3-HA3 with Sir4 from *sir2Δ* or *3Δ* cells (Fig. 5 B), indicating that stable Sir4 binding to Mps3 is dependent on other members of the SIR complex. However, Sir4 binding to Mps3 did not depend on yKu70, Esc1, or the myosin-like proteins Mlp1 and 2, which play a role in nuclear membrane organization, telomere length regulation, and SPB assembly (Strambio-de-Castillia et al., 1999; Hediger et al., 2002; Niepel, et al., 2005). The ability of Mps3 to bind to Sir4 in the absence of Esc1 suggests that Mps3 could be a novel nuclear receptor for silencing complexes at the nuclear periphery during S phase.

We observed a two-hybrid interaction between the Mps3 N terminus and a Sir4 fragment containing amino acids 839–1358 but not with a fragment containing amino acids 934–1358 (Fig. 5 C), indicating that amino acids 839–934 of Sir4 are required for Mps3 binding. This is adjacent to the predicted binding site of Esc1, which is located at amino acids 950–1262 (Andrulis et al., 2002), and overlaps the Sir2 binding site, which is located at amino acids 731–1358 (Cockell et al., 2000). We were unable to coimmunoprecipitate a bacterially expressed and purified Mps3 N terminus and Sir4 C terminus (unpublished data), suggesting that additional proteins such as Sir2 and 3, posttranslational modifications, and/or DNA itself are important for Mps3 binding to Sir4 in vitro.

Next, we wanted to examine the effect that the loss of Mps3 binding had on Sir4 localization in vivo. In 42% of wild-type cells enriched in S phase with hydroxyurea, Sir4 was present at multiple foci at the nuclear envelope (*n* = 100; Fig. 5 D). However, only 9% of *mps3Δ75–150* cells maintained this staining pattern (*n* = 100). Most *mps3Δ75–150* mutant cells contained an increased amount of Sir4 protein present in the diffuse nucleolar region that we frequently observed in the mutant (Fig. 5 D; unpublished data). Collectively, these data indicate that Mps3 interacts with Sir4 and functions to tether it throughout the nuclear periphery.

Chromosome recruitment using LexA-Sir4₈₃₉₋₉₃₄

To further demonstrate the importance of binding between the Mps3 acidic domain and amino acids 839–934 of Sir4, we took advantage of a chromatin localization assay to test if Sir4₈₃₉₋₉₃₄ could impart a specific localization to an otherwise randomly positioned chromosomal segment in an Mps3-dependent manner (Taddei et al., 2004a). We constructed a fusion between the coding sequence for amino acids 839–934 of Sir4, the LexA DNA-binding domain, and the nuclear localization sequence from SV40 large T antigen (*LexA-sir4₈₃₉₋₉₃₄*) and expressed it
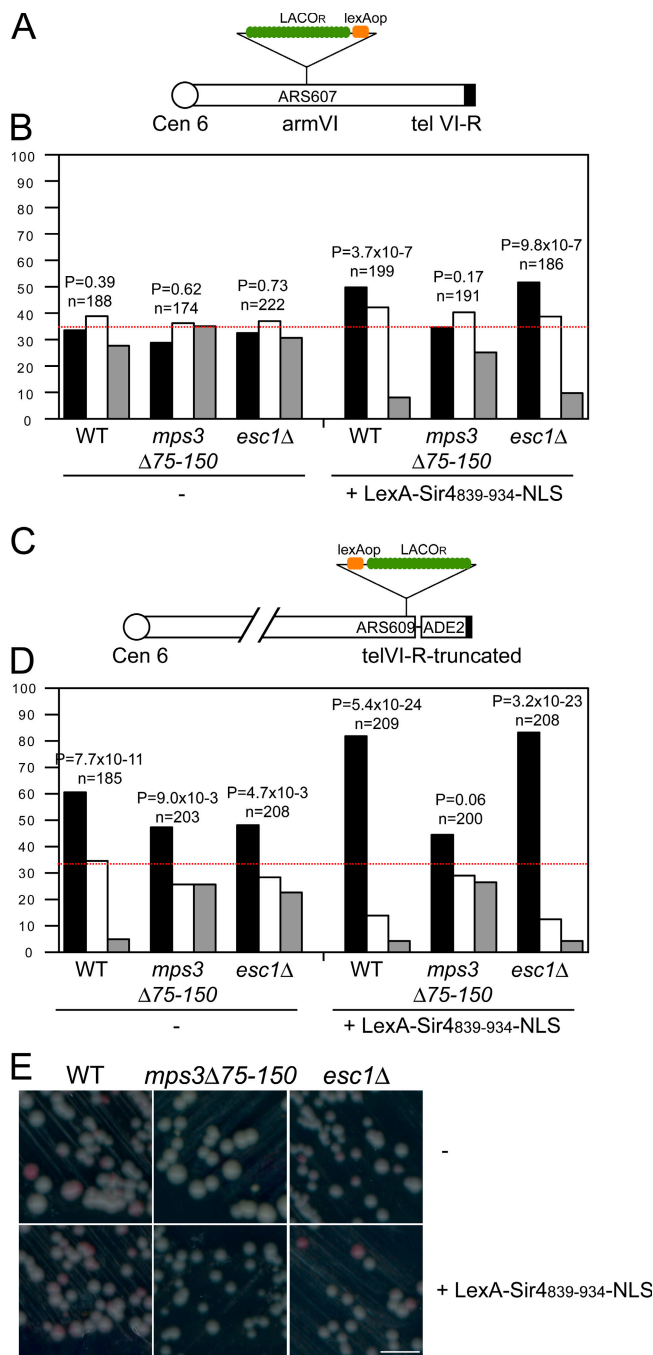
Figure 6. **LexA-Sir4$_{839-934}$ can recruit chromosomes to the nuclear periphery in the presence of the Mps3 acidic domain.** (A) Schematic of ~256 LacO$_R$ and four lexA^{op} binding sites integrated at ARS607, which is located on the arm of chromosome VI ~50 kb from the centromere and 70 kb from the telomere. (B) Wild-type, mps3Δ75–150, and esc1Δ cells that contained this version of chromosome VI as well as a galactose-inducible LexA-sir4$_{839-934}$-NLS (SLJ2651, SLJ2652, and SLJ2653, respectively) were grown overnight in YEP + 2% raffinose at 30°C to mid-log phase. Cultures were divided and 2% dextrose was added to repress expression (−) and 2% galactose was added to induce expression of LexA-sir4$_{839-934}$-NLS for 2 h at 30°C. Localization of arm VI to zone 1 (black), 2 (white), and 3 (gray) was then analyzed. The dotted line at 33% corresponds to a random distribution. Confidence values (P) for the χ^2 test were calculated for each dataset between random and test distributions. The number of cells examined in each dataset is indicated (n). (C) Schematic of ~256 LacO$_R$ and four lexA^{op} binding sites integrated at ARS609, near telomere VI-R. The subtelomeric sequence of telomere VI-R has also been truncated by the insertion of an ADE2 reporter linked to copies of the TG$_{1-3}$ telomeric repeats (Hediger

from the galactose-inducible GAL1 promoter in wild-type, mps3Δ75–150, and esc1Δ cells. These cells also contained four LexA operators (lexA^{op}) linked to tandem copies of the LacO$_R$ integrated into one of two loci on chromosome VI: the transcriptionally active ARS607 locus, which is located on the arm of chromosome VI >50 kb from either the centromere or the telomere (Fig. 6 A), or the subtelomeric ARS609 locus, 23 kb from telomere VI-R, which has been truncated by replacement of normal subtelomeric elements with an ADE2 reporter gene linked to terminal TG$_{1-3}$ telomeric repeats (Fig. 6 C; Hediger et al., 2002).

Analysis of chromosome position revealed that LexA-Sir4$_{839-934}$ was able to efficiently tether chromosome arm sequences to the nuclear periphery in wild-type and esc1Δ cells but not in mps3Δ75–150 mutants (Fig. 6 B). In addition, expression of LexA-sir4$_{839-934}$ was also able overcome the partial telomere tethering defect observed in esc1Δ mutants (Fig. 6 D; Taddei et al., 2004a), but it had no effect on mps3Δ75–150 cells, which also have a partial tethering defect of the truncated telomere VI-R (Fig. 6 D). This strongly suggests that amino acids 839–934 of Sir4 interact with the Mps3 acidic domain at the nuclear periphery and that the effects of this domain on chromosome recruitment to the membrane are independent of Esc1 binding.

Telomere silencing defects in mps3Δ75–150 mutants

These same strains contain an ADE2 marker that allowed us to determine if mps3Δ75–150 mutants have defects in transcriptional regulation of telomeric genes as a result of the loss of telomere tethering. Wild-type cells appeared as sectored red and white colonies after growth on plates containing limiting amounts of adenine caused by the stochastic expression of ADE2 (Fig. 6 E). ESC1 has previously been shown to be partially required for telomeric silencing (Andrulis et al., 2002; Taddei et al., 2004a), and, consistent with these reports, colonies harboring esc1Δ appeared light pink to white in color because of increased expression of ADE2 at the truncated telomere (Fig. 6 E). mps3Δ75–150 mutants also did not show sectoring, and colonies were light pink to white in color (Fig. 6 E), indicating that telomere silencing is decreased in cells lacking the Mps3 acidic domain. Furthermore, induction of LexA-sir4$_{839-934}$ was able to rescue the silencing defect of esc1Δ but not mps3Δ75–150 mutants (Fig. 6 E). Collectively, these results demonstrate that defects in telomere tethering in mps3Δ75–150 mutants are directly correlated with effects on telomeric gene expression; the fact that neither can be rescued by LexA-sir4$_{839-934}$ strongly suggests

et al., 2002). (D) Localization of truncated telomere VI-R in wild-type, mps3Δ75–150, and esc1Δ cells that contained a galactose-inducible LexA-sir4$_{839-934}$-NLS (SLJ2647, SLJ2648, and SLJ2649, respectively), determined as described in B. (E) Expression of the telomeric ADE2 gene in strains from D was monitored by streaking cells to SD plates containing 10 μg/ml adenine and 2% dextrose or 2% galactose/2% raffinose to repress (−) or induce the expression of LexA-sir4$_{839-934}$-NLS, respectively. After growth for 3 d at 30°C, plates were incubated for 1 wk at 4°C to allow the red pigment to develop. Expression of ADE2 results in white colored cells and blocks the accumulation of the red pigment in this strain background; this occurs in cells that have lost telomeric silencing. Bar, 1 cm.
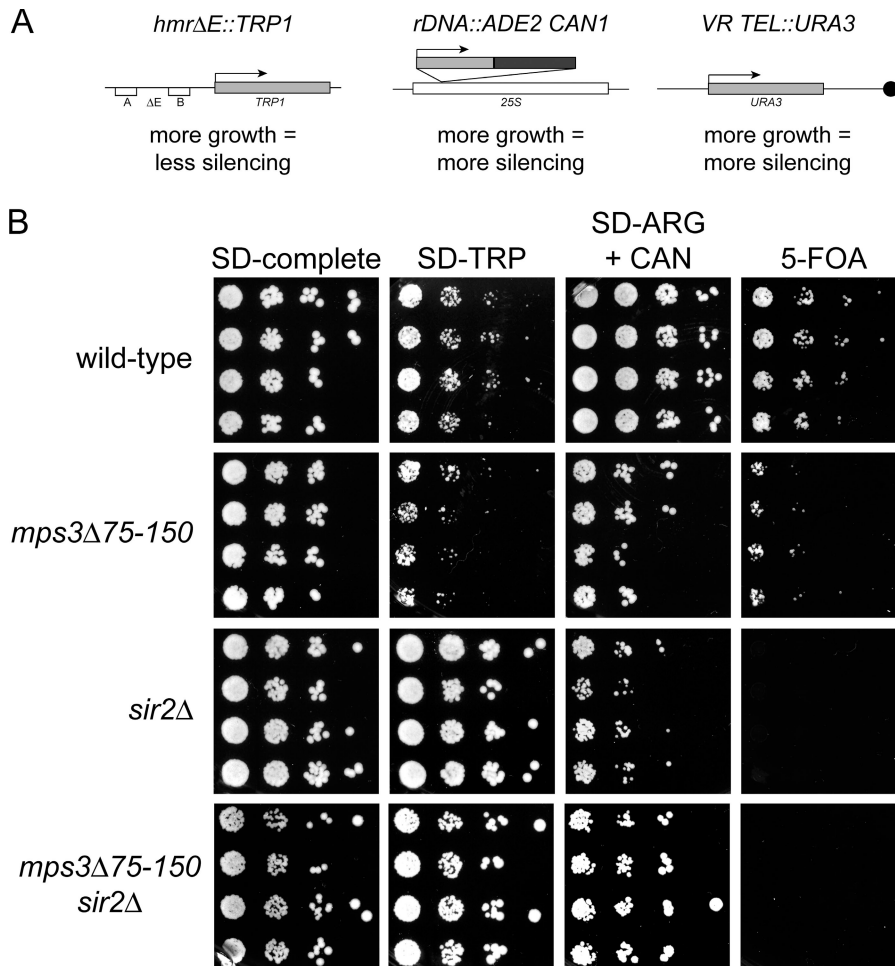
A

hmrΔE::TRP1

more growth =
less silencing

rDNA::ADE2 CAN1

more growth =
more silencing

VR TEL::URA3

more growth =
more silencing

B

	SD-complete	SD-TRP	SD-ARG + CAN	5-FOA
wild-type				
mps3Δ75-150				
sir2Δ				
mps3Δ75-150 sir2Δ				

Figure 7. **mps3Δ75–150 mutants are defective in telomeric silencing.** (A) Three different reporter genes are present in the triple silencer strain to allow simultaneous monitoring of silencing at the mating-type locus, rDNA, and telomeres (Ray et al., 2003). Expression of *TRP1* in the *HMR* locus, which contains a deletion in the E element of the *E* silencer, is monitored by growth on medium lacking tryptophan, where more growth equals less silencing. The expression of *CAN1* in the rDNA locus was monitored using negative selection against *CAN1* expression so that more growth equals more silencing. Expression of *URA3* placed adjacent to the right telomere of chromosome V (indicated by the black dot) is monitored by negative selection on 5-FOA so that more growth equals more silencing. Arrows indicate the direction of transcription of each reporter gene. (B) 10-fold serial dilutions of single yeast colonies of the indicated genotype were spotted onto different media at 30°C. Representative colonies from four assays are shown. SD complete medium shows the total number of cells spotted and the other media (SD-TRP, SD-ARG + CAN, and 5-FOA) show the extent of silencing at *HMR*, rDNA, and telomere V-R, respectively. Because the *CAN1* reporter in the rDNA locus represents a single gene in an array of 100−150 genes, small changes in growth are considered to represent a larger change in silencing compared with the *HMR* and telomere reporters, which comprise the entire locus (Ray et al., 2003).

that the interaction between the Mps3 N terminus and Sir4 is important for telomere tethering and the telomere position effect.

In addition to telomeres, the mating-type loci and the ribosomal DNA (rDNA) locus are also silenced from transcription by RNA polymerase II. We analyzed transcriptional regulation at these loci in *mps3Δ75–150* mutants using a strain containing reporter constructs to allow simultaneous detection of expression at telomere V-R, the silent mating-type locus *HMR*, and the rDNA (Fig. 7 A; Ray et al., 2003). Consistent with our telomere VI-R findings, we observed derepression of *URA3* integrated at telomere V-R in *mps3Δ75–150* mutants, resulting in decreased growth on plates containing the suicide substrate 5-FOA (Fig. 7 B). Interestingly, we also observed a decrease in silencing at the rDNA locus in *mps3Δ75–150* cells, whereas repression at *HMR* was increased ∼10-fold (Fig. 7 B). The silencing defects observed in *mps3Δ75–150* mutants are not as great as in *sir2Δ* cells, but the fact that *mps3Δ75–150 sir2Δ* double mutants do not have additive effects on silencing is consistent with the possibility that Mps3 and Sir2 are in the same pathway of transcriptional repression (Fig. 7 B).

Expression of the Mps3 N-terminal fragments *mps3 1–150* and *mps3 1–181* was able to restore telomere tethering at the nuclear periphery in *mps3Δ75–150* mutants. We also found that when we expressed either *mps3 1–150* or *mps3 1–181* from the *MPS3* promoter on a 2-μm plasmid in *mps3Δ75–150* cells, it was

sufficient to restore silencing at *HMR*, rDNA, and telomere V-R to similar levels observed in the wild type (Fig. 8). Therefore, the Mps3 N terminus is necessary and sufficient for both telomere tethering and the telomere position effect.

Discussion

In this paper, we have shown that the SUN protein Mps3 plays a role in the telomere position effect and telomere tethering at the nuclear periphery through the interaction of its N-terminal acidic domain with Sir4. As the first integral membrane protein in budding yeast known to play a role in chromosome positioning during mitotic growth, Mps3 could function to regulate chromatin structure or simply act as a DNA tether at the nuclear periphery. Based on the ability of LexA-sir4₈₃₉₋₉₃₄ to recruit both telomeric as well as actively transcribed chromosome arm DNA to the nuclear membrane in an Mps3- dependent manner, we propose that the primary function of Mps3 is to be a DNA/chromatin anchor. Additional support for this hypothesis comes from recent findings that *mps3-3* mutants fail to cluster telomeres at the nuclear periphery (Antoniacci et al., 2007), of the role of Mps3 in formation of the meiotic bouquet (Conrad et al., 2007), and of the fact that the N terminus lacks any motifs of functional significance that would suggest a role in chromatin assembly (Jaspersen et al., 2006).

Figure 8. **The Mps3 N terminus is able to rescue the silencing defect of *mps3Δ75–150* mutants.** A 2-μm plasmid containing no insert, *MPS3*, *mps3 1–75*, *mps3 1–150*, or *mps3 1–181* was transformed into the *mps3Δ75–150* mutant (SLJ2516), and silencing at telomere V-R, *HMR*, and the rDNA was assayed as described in Fig. 7.
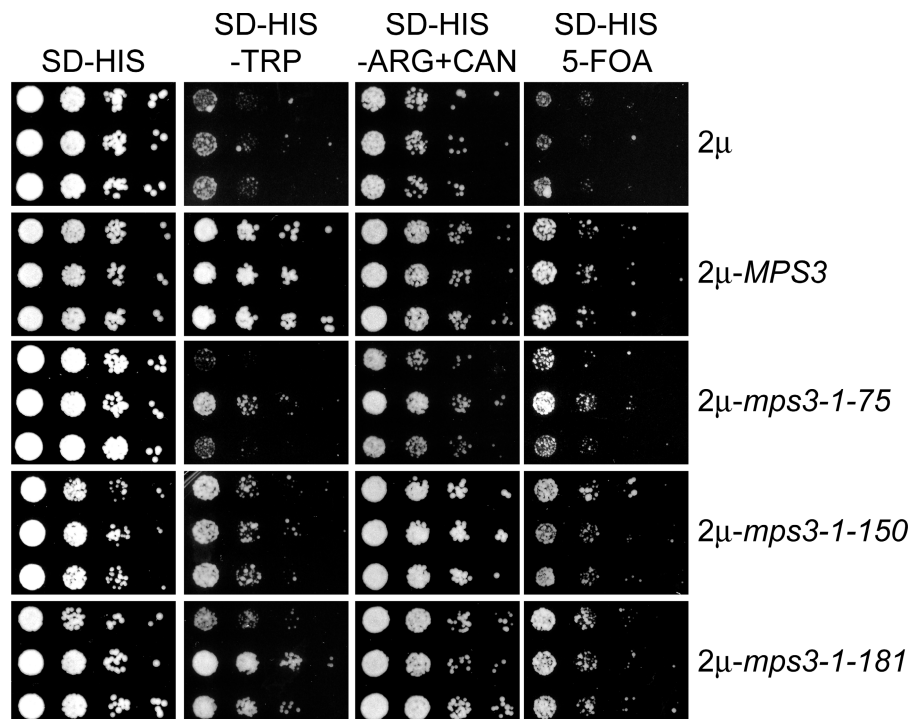
Based on our chromosome recruitment studies with LexA-sir4839–934, we currently favor a model in which Mps3 does not directly bind DNA but rather associates with chromosomes via interaction of the N terminus with other proteins, including Sir4. Binding to chromatin-associated proteins such as Sir4 would allow Mps3 to recognize particular chromosome domains for selective tethering at the nuclear periphery. Given that we were unable to coimmunoprecipitate recombinant Mps3 and Sir4, it seems likely that the interaction between the Mps3 N terminus and Sir4 is facilitated by additional proteins or chromatin. Obvious candidates include Sir2 and 3 because binding between Mps3 and Sir4 in vivo was dependent on both of these proteins. Other candidates include the telomere elongation factor Est1, the establishment of cohesion protein Eco1/Ctf7, the protein kinase Cdc5, and the histone 2A variant Htz1, all of which are chromosome-interacting proteins that bind to Mps3 in the two-hybrid system (Uetz et al., 2000; Antoniacci et al., 2004; Antoniacci et al., 2007).

The silencing factors Sir2, 3, and 4 are present in limiting concentrations in the yeast nucleus except at the telomeres (Buck and Shore, 1995; Maillet et al., 1996; Marcand et al., 1996). Localization of silencing proteins as well as telomeres to the nuclear periphery is thought to create a subcompartment of the nucleus that favors silencing and protects the rest of the genome from aberrant transcriptional repression by the SIRs (for review see Akhtar and Gasser, 2007). Binding of Sir4 to Mps3 at the nuclear membrane could be an early step in the formation of silent heterochromatin at the telomeres, although Mps3 also may associate with telomere binding proteins to directly mediate recruitment of chromosome ends to the periphery (Antoniacci and Skibbens, 2006). Consistent with a role in recruitment of Sir4 and/or telomeres at the nuclear periphery, we observed a loss of telomeric silencing in *mps3Δ75–150* mutants. However, the

fact that we also did not observe a decrease in silencing at *HMR* indicates that the Mps3 N terminus does not play an integral role in silencing per se by altering chromatin structure but rather is additional evidence for our hypothesis that Mps3 is a nuclear envelope anchor. Increased silencing at the mating type loci in *mps3Δ75–150* mutants is likely caused by dissociation of SIR proteins from telomeres followed by their redistribution to internal chromosomal sites such as *HML* and *HMR*, as has been observed previously for other mutants in telomere and SIR tethering (Martin et al., 1999; Hediger et al., 2002; Taddei et al., 2004a). Our analysis of Sir4 staining demonstrates that at least one component of the SIR complex is relocalized in *mps3Δ75–150* mutants. However, the effects that this change in localization has on DNA binding of Sir4 and other components of the SIR complex at a molecular level are currently unknown.

Interaction between Mps3 and chromatin-associated proteins including Sir4 is likely important for proper localization of Mps3 to the inner nuclear membrane because Mps3 lacks any nuclear targeting information (Lusk et al., 2007). Loss of binding to nuclear proteins would result in a lack of Mps3 retention in the peripheral nuclear envelope; this is the phenotype we observed with *mps3Δ75–150–GFP*. The fact that Mps3 N-terminal fragments are able to restore both telomere positioning and silencing suggests that they contain information sufficient for nuclear localization, either through binding to *mps3Δ75–150* protein still present in the cell or nuclear localization information present within the N-terminal fragments themselves. Localization of other SUN proteins to the inner nuclear envelope requires determinants in both the N- and C-terminal regions and in many cases involves interaction between the SUN protein and nuclear proteins, such as the lamins (Padmakumar et al., 2005; Starr and Fischer, 2005; Crisp et al., 2006; Haque et al., 2006; Hasan et al., 2006; Wang et al., 2006; Liu et al., 2007).

Isolation and characterization of *mps3Δ75–150* mutants indicates that the role of Mps3 in telomere positioning and gene regulation is separable from its function at the SPB. In addition, the fact that different regions of the Mps3 N terminus and distinct Mps3 binding partners appear to be required for mitotic versus meiotic telomere tethering (Conrad et al., 2007) strongly suggests that distinct mechanisms of chromosome positioning likely exist during the different growth phases. The involvement of Mps3 in telomere tethering during both vegetative and meiotic growth raises the interesting possibility that other SUN proteins will also play a role in chromosome positioning during mitotic growth. Given the known connection between SUN proteins and the cytoskeleton, an additional interaction with chromatin could represent a novel mechanism of communication between the cytoplasm and the nucleus that does not require transport through the nuclear pore complex.

Materials and methods

Yeast strains and plasmids
All strains are derivatives of W303 (*ade2-1, trp1-1, leu2-3,112, ura3-1, his3-11,15,* and *can1-100*) and are listed in Table S1 (available at http://www.jcb.org/cgi/content/full/jcb.200706040/DC1). Standard techniques were used for DNA and yeast manipulations.

Deletions in the *MPS3* N terminus were constructed in pSJ148 (pRS305-*MPS3*) by introducing in-frame NheI restriction sites to remove to the corresponding coding sequence after digestion and religation. Wild-type and mutant forms were digested with BstEII to direct integration into the *LEU2* locus of SLJ2039 and single copy integration was verified by Southern blotting.

N-terminal truncation mutants in *MPS3* were created in pRS306 and pRS423 by PCR amplification of the indicated region of the *MPS3* open reading frame along with ~800 bp of promoter as XhoI–BamHI fragments. Plasmids were digested with XcmI to target integration to *URA3* or were directly transformed into yeast.

To create pRS306–*MPS3-GFP* and pRS306–*mps3Δ75–150–GFP*, the coding sequence for GFP was first amplified by PCR and inserted into the XbaI–SacI sites of pRS306. *MPS3* and *mps3Δ75–150*, including ~800 bp of promoter sequence, were then amplified by PCR and ligated in frame to the GFP at the KpnI–BamHI sites. Both plasmids were digested with EcoRV to direct integration into the *URA3* locus of a diploid strain containing *mps3Δ–NATMX*. Haploid strains were recovered by sporulation.

Constructs for two-hybrid analysis were made by PCR amplification of the indicated regions of *MPS3* and *SIR4* with primers containing NcoI and XhoI ends. After digestion, the products were cloned into the NcoI–SalI sites of pOAD1 or pOBD2 (Uetz et al., 2000). pOAD1 plasmids were transformed into the prey strain SLJ1644, and pOBD2 plasmids were transformed into the bait strain SLJ1645.

The LexA DNA-binding domain was amplified by PCR as a XhoI–NcoI fragment and ligated into pSJ100, a plasmid derived from pRS303 containing the *GAL1/10* promoter at KpnI–XhoI, LacI at BamHI, and SV40 NLS at BamHI–XbaI. Next, the region of *SIR4* encoding amino acids 839–934 was amplified as a NcoI–BglII fragment and cloned into the NcoI–BamHI sites of the previous vector. The entire *GAL-LexA-sir4$_{839–934}$-NLS* insert was then moved into pRS306 using KpnI–SacI to create pRS306-*GAL-LexA-sir4$_{839–934}$-NLS*, which was digested with StuI to target integration into the *URA3* locus.

Cytological techniques
Analyses of DNA content by flow cytometry and protein localization by indirect immunofluorescence and epifluorescence microscopy were performed as described previously (Jaspersen et al., 2002, 2006). The following primary antibody dilutions were used: 1:500 rat anti-tubulin YOL1/34 (Accurate Chemical and Scientific Corporation), 1:500 affinity purified rabbit anti-Tub4 (Jaspersen et al., 2002), and 1:1,000 goat anti-Sir4 (Santa Cruz Biotechnology, Inc.) antibodies. Secondary antibodies included 1:10,000 Cy3-conjugated goat anti–rabbit IgG (Millipore), 1:200 fluorescein-conjugated goat anti–rat IgG (Millipore), and 1:10,000 Alexa 555–conjugated donkey anti–goat IgG (Invitrogen). DNA was visualized by staining with 1 μg/ml

DAPI for 5 min immediately before mounting with Citifluor (Ted Pella, Inc.). Cells were examined at room temperature with an imaging system (Axio-Imager; Carl Zeiss, Inc.) using a 100× α-Plan Fluar objective (NA 1.45; Carl Zeiss, Inc.), and images were captured with a digital camera (Orca ER; Hamamatsu) and processed using Axiovision 4.6.3 (Carl Zeiss, Inc.). Constrained iterative deconvolution was used to generate the images presented in Fig. 5 D whereas images in Fig. 1 D are single z section slices.

To analyze nuclear envelope staining of Mps3-GFP, cells were grown to mid-log phase in synthetic complete media supplemented with 5× adenine and placed onto 25% gelatin pads as described previously (Maddox et al., 2000). Imaging was performed on a laser scanning microscope (LSM 510 META; Carl Zeiss, Inc.) equipped with a ConfoCor3 module with avalanche photodiode detectors (Carl Zeiss, Inc.) using a 100× α-Plan Fluar lens (NA 1.45) at room temperature. Excitation of Mps3-GFP was performed with a 488-nm Argon laser line and the appropriate filter sets. Data was acquired using AIM software (Carl Zeiss, Inc.). High resolution volume renderings of the acquired three-dimensional images were generated using software (Velocity 4.0; Improvision) and projected as two-dimensional images in Fig. 1 (F and G).

The position of GFP spots was determined as described previously (Hediger et al., 2002; Taddei et al., 2004a). In brief, an imaging system (AxioImager) with a 100× α-Plan Fluar objective (NA 1.45) and a digital camera (Orca ER) were used to capture 19-image stacks of 170-nm step size through nuclei of log-phase cells at room temperature. The spot-to-periphery distance and nuclear diameter were determined in a single z stack image where the spot was most concentrated using Axiovision 4.6.3, except in cases when the spot fell into one of the top or bottom three focal planes. By dividing the spot-to-periphery distance by the diameter, each spot fell into one of three zones of equal surface (Fig. 2 A). Zone 1 has a width of 0.184 × the nuclear radius (r), zone 2 has a width of 0.184–0.422 × r, and zone 3 has a width of 0.422 × r. Confidence values (P) for the χ^2 test were calculated for each dataset between random and test distributions.

Immunoprecipitation and Western blotting
Liquid nitrogen ground lysates were prepared from 500 OD$_{600}$ of mid-log phase cells as described previously (Jaspersen et al., 2006). 50 μl of anti-HA resin (Roche) was added to lysates to immunoprecipitate Mps3-HA3. After 2 h of incubation at 4°C, beads were washed five times and 1/10 of the bound protein was analyzed by SDS-PAGE followed by Western blotting.

The following primary antibody dilutions were used: 1:1,000 anti-HA 16B12 (Covance), 1:1,000 anti-GFP B34 (Covance), 1:2,000 anti-glucose-6-phosphate dehydrogenase (Sigma-Alrich), and 1:1,000 anti-Sir4 (Santa Cruz Biotechnology, Inc.). Alkaline phosphatase–conjugated secondary antibodies were used at 1:10,000 (Promega).

Online supplemental material
Table S1 shows yeast strains used. Online supplemental material is available at http://www.jcb.org/cgi/content/full/jcb.200706040/DC1.

References

Akhtar, A., and S.M. Gasser. 2007. The nuclear envelope and transcriptional control. *Nat. Rev. Genet.* 8:507–517.

Andrulis, E.D., A.M. Neiman, D.C. Zappulla, and R. Sternglanz. 1998. Perinuclear localization of chromatin facilitates transcriptional silencing. *Nature.* 394:592–595.

Andrulis, E.D., D.C. Zappulla, A. Ansari, S. Perrod, C.V. Laiosa, M.R. Gartenberg, and R. Sternglanz. 2002. Esc1, a nuclear periphery protein required for Sir4-based plasmid anchoring and partitioning. *Mol. Cell. Biol.* 22:8292–8301.

Antoniacci, L.M., and R.V. Skibbens. 2006. Sister-chromatid telomere cohesion is nonredundant and resists both spindle forces and telomere motility. *Curr. Biol.* 16:902–906.

Antoniacci, L.M., M.A. Kenna, P. Uetz, S. Fields, and R.V. Skibbens. 2004. The spindle pole body assembly component Mps3p/Nep98p functions in sister chromatid cohesion. *J. Biol. Chem.* 279:49542–49550.

Antoniacci, L.M., M.A. Kenna, and R.V. Skibbens. 2007. The nuclear envelope and spindle pole body-associated Mps3 protein bind telomere regulators and function in telomere clustering. *Cell Cycle.* 6:75–79.

Buck, S.W., and D. Shore. 1995. Action of a *RAP1* carboxy-terminal silencing domain reveals an underlying competition between *HMR* and telomeres in yeast. *Genes Dev.* 9:370–384.

Chikashige, Y., C. Tsutsumi, M. Yamane, K. Okamasa, T. Haraguchi, and Y. Hiraoka. 2006. Meiotic proteins bqt1 and bqt2 tether telomeres to form the bouquet arrangement of chromosomes. *Cell.* 125:59–69.

Cockell, M.M., S. Perrod, and S.M. Gasser. 2000. Analysis of Sir2p domains required for rDNA and telomeric silencing in *Saccharomyces cerevisiae. Genetics.* 154:1069–1083.

Conrad, M.N., C.-Y. Lee, J.L. Wilkerson, and M.E. Dresser. 2007. *MPS3* mediates meiotic bouquet formation in *Saccharomyces cerevisiae. Proc. Natl. Acad. Sci. USA.* 104:8863–8868.

Crisp, M., Q. Liu, K. Roux, J.B. Rattner, C. Shanahan, B. Burke, P.D. Stahl, and D. Hodzic. 2006. Coupling of the nucleus and cytoplasm: role of the LINC complex. *J. Cell Biol.* 172:41–53.

Ding, X., R. Xu, J. Yu, T. Xu, Y. Zhuang, and M. Han. 2007. SUN1 is required for telomere attachment to the nuclear envelope and gametogenesis in mice. *Dev. Cell.* 12:863–872.

Fraser, P., and W. Bickmore. 2007. Nuclear organization of the genome and the potential for gene regulation. *Nature.* 447:413–417.

Gartenberg, M.R., F.R. Neumann, T. Laroche, M. Blaszczyk, and S.M. Gasser. 2004. Sir-mediated repression can occur independently of chromosomal and subnuclear contexts. *Cell.* 119:955–967.

Gotta, M., T. Laroche, A. Formenton, L. Maillet, H. Scherthan, and S. Gasser. 1996. The clustering of telomeres and colocalization with Rap1, Sir3, and Sir4 proteins in wild-type *Saccharomyces cerevisiae. J. Cell Biol.* 134:1349–1363.

Gottschling, D.E., O.M. Aparicio, B.L. Billington, and V.A. Zakian. 1990. Position effect at *S. cerevisiae* telomeres: reversible repression of PolII transcription. *Cell.* 134:751–762.

Haque, F., D.J. Lloyd, D.T. Smallwood, C.L. Dent, C.M. Shanahan, A.M. Fry, R.C. Trembath, and S. Shackleton. 2006. SUN1 interacts with nuclear lamin A and cytoplasmic nesprins to provide a physical connection between the nuclear lamina and the cytoskeleton. *Mol. Cell. Biol.* 26:3738–3751.

Hasan, S., S. Guttinger, P. Muhlhausser, F. Anderegg, S. Burgler, and U. Kutay. 2006. Nuclear envelope localization of human UNC84A does not require nuclear lamins. *FEBS Lett.* 580:1263–1268.

Hediger, F., F.R. Neumann, G. Van Houwe, K. Dubrana, and S.M. Gasser. 2002. Live imaging of telomeres: yKu and Sir proteins define redundant telomere-anchoring pathways in yeast. *Curr. Biol.* 12:2076–2089.

Jaspersen, S.L., T.H. Giddings Jr., and M. Winey. 2002. Mps3p is a novel component of the yeast spindle pole body that interacts with the yeast centrin homologue Cdc31p. *J. Cell Biol.* 159:945–956.

Jaspersen, S.L., A.E. Martin, G. Glazko, T.H. Giddings Jr., G. Morgan, A. Mushegian, and M. Winey. 2006. The Sad1-UNC-84 homology domain in Mps3 interacts with Mps2 to connect the spindle pole body with the nuclear envelope. *J. Cell Biol.* 174:665–675.

Liu, Q., N. Pante, T. Misteli, M. Elsagga, M. Crisp, D. Hodzic, B. Burke, and K.J. Roux. 2007. Functional association of Sun1 with nuclear pore complexes. *J. Cell Biol.* 178:785–798.

Lusk, C.P., G. Blobel, and M.C. King. 2007. Highway to the inner nuclear membrane: rules for the road. *Nat. Rev. Mol. Cell Biol.* 8:414–420.

Maddox, P.S., K.S. Bloom, and E.D. Salmon. 2000. The polarity and dynamics of microtubule assembly in the budding yeast *Saccharomyces cerevisiae. Nat. Cell Biol.* 2:36–41.

Maillet, L., C. Boscheron, M. Gotta, S. Marcand, E. Gilson, and S.M. Gasser. 1996. Evidence for silencing compartments within the yeast nucleus: a role for telomere proximity and Sir protein concentration in silencer-mediated repression. *Genes Dev.* 10:1796–1811.

Maillet, L., F. Gaden, V. Brevet, G. Fourel, S.G. Martin, K. Dubrana, S.M. Gasser, and E. Gilson. 2001. Ku-deficient yeast strains exhibit alternative states of silencing competence. *EMBO Rep.* 2:203–210.

Marcand, S., S.W. Buck, P. Moretti, E. Gilson, and D. Shore. 1996. Silencing of genes at nontelomeric sites in yeast is controlled by sequestration of silencing factors at telomeres by Rap1 protein. *Genes Dev.* 10:1297–1309.

Martin, S.G., T. Laroche, N. Suka, M. Grunstein, and S.M. Gasser. 1999. Relocalization of telomeric Ku and SIR proteins in response to DNA strand breaks in yeast. *Cell.* 97:621–633.

Moazed, D., A.D. Rudner, J. Huang, G.J. Hoppe, and J.C. Tanny. 2004. A model for step-wise assembly of heterochromatin in yeast. *Novartis Found. Symp.* 259:48–62.

Niepel, M., C. Strambio-de-Castillia, J. Fasolo, B.T. Chait, and M.P. Rout. 2005. The nuclear pore complex–associated protein, Mlp2p, binds to the yeast spindle pole body and promotes its efficient assembly. *J. Cell Biol.* 170:225–235.

Nishikawa, S., Y. Terazawa, T. Nakayama, A. Hirata, T. Makio, and T. Endo. 2003. Nep98p is a component of the yeast spindle pole body and essential for nuclear division and fusion. *J. Biol. Chem.* 278:9938–9943.

Padmakumar, V.C., T. Libotte, W. Lu, H. Zaim, S. Abraham, A.A. Noegel, J. Gotzmann, R. Foisner, and I. Karakesisoglou. 2005. The inner nuclear membrane protein Sun1 mediates the anchorage of Nesprin-2 to the nuclear envelope. *J. Cell Sci.* 118:3419–3430.

Penkner, A., L. Tang, M. Novatchkova, M. Ladurner, A. Fridkin, Y. Gruenbaum, D. Schweizer, J. Loidl, and V. Jantsch. 2007. The nuclear envelope protein Matefin/SUN-1 is required for homologous pairing in *C. elegans* meiosis. *Dev. Cell.* 12:873–885.

Ray, A., R.E. Hector, N. Roy, J.-H. Song, K.L. Berkner, and K.W. Runge. 2003. Sir3p phosphorylation by the Slt2p pathway effects redistribution of silencing function and shortened lifespan. *Nat. Genet.* 33:522–526.

Rusche, L.N., A.L. Kirchmaier, and J. Rine. 2003. The establishment, inheritance, and function of silenced chromatin in *Saccharomyces cerevisiae. Annu. Rev. Biochem.* 72:481–516.

Schmitt, J., R. Benavente, D. Hodzic, C. Hoog, C.L. Stewart, and M. Alsheimer. 2007. Transmembrane protein Sun2 is involved in tethering mammalian meiotic telomeres to the nuclear envelope. *Proc. Natl. Acad. Sci. USA.* 104:7426–7431.

Starr, D.A., and J.A. Fischer. 2005. KASH 'n Karry: the KASH domain family of cargo-specific cytoskeletal adaptor proteins. *Bioessays.* 27:1136–1146.

Strambio-de-Castillia, C., G. Blobel, and M.P. Rout. 1999. Proteins connecting the nuclear pore complex with the nuclear interior. *J. Cell Biol.* 144:839–855.

Taddei, A., F. Hediger, F.R. Neumann, C. Bauer, and S.M. Gasser. 2004a. Separation of silencing from perinuclear anchoring functions in yeast Ku80, Sir4 and Esc1 proteins. *EMBO J.* 23:1301–1312.

Taddei, A., F. Hediger, F.R. Neumann, and S.M. Gasser. 2004b. The function of nuclear architecture: a genetic approach. *Annu. Rev. Genet.* 38:305–345.

Tang, X., Y. Jin, and W.Z. Cande. 2006. Bqt2p is essential for initiating telomere clustering upon pheromone sensing in fission yeast. *J. Cell Biol.* 173:845–851.

Tzur, Y.B., K.L. Wilson, and Y. Gruenbaum. 2006. SUN-domain proteins: 'Velcro' that links the nucleoskeleton to the cytoskeleton. *Nat. Rev. Mol. Cell Biol.* 7:782–788.

Uetz, P., L. Giot, G. Cagney, T.A. Mansfield, R.S. Judson, J.R. Knight, D. Lockshon, V. Narayan, M. Srinivasan, P. Pochart, et al. 2000. A comprehensive analysis of protein-protein interactions in *Saccharomyces cerevisiae. Nature.* 403:623–627.

Wang, Q., X. Du, Z. Cai, and M.I. Greene. 2006. Characterization of the structures involved in localization of the SUN proteins to the nuclear envelope and the centrosome. *DNA Cell Biol.* 25:554–562.

Worman, H.J., and G.G. Gundersen. 2006. Here come the SUNs: a nucleocytoskeletal missing link. *Trends Cell Biol.* 16:67–69.